DOI 10.7343/as-2023-667

ACQUE SOTTERRANEE
Italian Journal of Groundwater

2023-AS45-667: 77- 90

journal homepage: https://www.acquesotterranee.net/

The integration of geochemical and isotopic approaches for thermo-mineral water characterization: the case of Tebessa (North Eastern Algeria)

Caratterizzazione delle acque termominerali di Tebessa mediante approcci geochimici ed isotopici: il caso di studio di Tebessa (nord-est dell'Algeria)

Yacine LEKRINE[a], Abdeslam DEMDOUM[b], Foued BOUAICHA [c]

[a] Laboratory of Geology and Environment (LGE), Université Constantine 1, Constantine 025000, Algeria. Email: *hydro.yacin@gmail.com*

[b] Department of Earth Sciences, University of Setif 1, Setif 19000 Algeria. Email : *slimdem@yahoo.fr*

[c] Department of applied biology, Université Constantine 1, Constantine 025000, Algeria. Email : *bouaicha.foued@umc.edu.dz*;
Tel: (+213) 06 70 30 45 70

ARTICLE INFO

Ricevuto/*Received*: 30 March 2023
Accettato/*Accepted*: 22 June 2023
Pubblicato online/*Published online*: 30 June 2023

Handling Editor:
Stefano Viaroli

Citation:
Lekrine, Y., Demdoum, A., Bouaicha, F. (2023). The integration of geochemical and isotopic approaches for thermo-mineral water characterization: the case of Tebessa (North Eastern Algeria). Acque Sotterranee - *Italian Journal of Groundwater*, 12(2), 77 - 90
https://doi.org/10.7343/as-2023-667

Correspondence to:
Foued Bouaicha
bouaicha.foued@umc.edu.dz

Keywords: *thermo-mineral water, multivariate analysis, geochemical modeling, stable isotopes, Tebessa, Algeria.*

Parole chiave: acque termo-minerali, analisi multivariata, modellazione geochimica, isotopi stabili, Tebessa, Algeria

Riassunto

Questa ricerca si propone come obiettivo la valutazione dell'evoluzione idrogeochimica e la valutazione per l'uso potabile e irriguo delle sorgenti dall'acquifero alluvionale e dai principali sistemi acquiferi carsici a Tebessa (settore nord-orientale dell'Algeria). Per raggiungere questo obiettivo, 25 campioni di acque sotterranee provenienti da diverse sorgenti, comprese le sorgenti termominerali, sono stati esaminati e sottoposti ad analisi statistica multivariata (analisi delle componenti principali), analisi isotopiche e modellazione geochimica. È stato individuato che le acque sotterranee calde interagiscono in profondità con le evaporiti triassiche lungo i piani di faglia, dando origine a delle acque di tipo Cloruro sodica. Inoltre, l'acqua della falda carsica é di tipo Bicarbonatico - calcica con bassa salinità. Nell'area di studio, due facies chimiche sono predominanti: Ca^{2+}- HCO_3^- and Na^+- Cl^-. La maggior parte dei cationi e degli anioni e della conduttività elettrica delle sorgenti, sono al di sotto dei limiti consentiti per l'acqua potabile. L'interazione acqua-roccia, soprattutto la dissoluzione di carbonati e silicati, svolge un ruolo principale nella composizione chimica delle acque sotterranee. Le analisi isotopiche di $\delta^{18}O$ e δ^2H delle acque suggeriscono che le acque non termali nell'area di studio siano di origine meteorica. L'acquifero si ricarica dalle precipitazioni che avvengono in un'area più elevata (600-1700 m) tramite l'infitrazionne attraverso faglie e fratture nelle formazioni carbonatiche del Monte Tebessa.

Abstract

This research aims to assess the hydrogeochemical evolution and the assessment for drinking and irrigation use of the spring water from the alluvial aquifer and major karst aquifer systems in Tebessa (the northeastern part of Algeria). For achieving this goal, 25 groundwater samples from several springs, including thermo-mineral springs, were examined and subjected to multivariate statistical analysis (principal component analysis), isotopic approaches, and geochemical modelling. However, it was revealed that the hot waters interact at depth with Triassic evaporates located in the hydrothermal conduit (fault), giving rise to the Na^+-Cl^- water type. Furthermore, the freshwater characterized the karst aquifer marked by the Ca^{2+} HCO_3^- water type with low salinity concentrations. On the other hand, the majority of cations and anions and electrical conductivity, which characterize the chemical composition of the overall water springs, were below the limits allowed for drinking water according to the standards. In terms of hydrochemical facies, it was discovered that throughout the study area, two chemical facies were predominant (Ca^{2+}- HCO_3^- and Na^+- Cl^-). Water-rock interaction, characterized by the dissolution of carbonates and silicates, plays a primordial role in the chemical composition of the groundwater. Stable isotopic analyses of the $\delta^{18}O$ and δ^2H compositions of the waters suggest that the cold waters of the study area are of meteoric origin. Anyway, it was concluded that the meteoric recharge was precipitation, which recharged from a higher altitude (600–1700 m) and infiltrated through deep faults and fractures in the carbonate formations of the Tebessa Mount.

Introduction

Water is a vital for all life on Earth; though water covered 80% of the surface of the earth, the freshwater supply has increasingly become a limiting factor. Groundwater is the most important natural resource used for drinking by many people around the world, especially in arid and semi-arid areas (Karami et al., 2018; Loh et al., 2020). In the Tebessa region, the most common source of drinking water for the inhabitants is springs and wells. They are considered the main source of water available for the settlements of Hammamet, Tebessa, and Morsott (Fehdi et al., 2009). These water supplies are an important public health issue because they are often vulnerable and may cause microbiological or chemical quality-associated health risks water consumers. Therefore, the quality control of natural springs and well water is an area of interest. As a result, the quality of groundwater in the study area is largely determined by natural processes and human activities (Rouabhia et al., 2010; Sedrati & Djabri, 2014; Zereg et al., 2018).

Over the past decades, statistical and computational advanced methods have been developed to classify large clusters of data within a significant range, extract useful information, identify the relationships between the corresponding data and assess the results. While numerous methods such as multivariate statistical techniques have made it possible for better and easier evaluation for the interpretation of complex data in water quality studies (Călmuc et al., 2018; Drias et al., 2020; Fehdi et al., 2016). Likewise, another study stated that multivariate statistical techniques are useful for reducing the voluminous data obtained from physico-chemical water quality studies (Giri et al., 2019). Therefore, the present study was undertaken to identify important factors in a large data set significantly affecting the quality of water springs (Chelih et al., 2018; Chemseddine et al., 2015). The application of multivariate statistical techniques reveals relationships using analytical techniques such as hierarchical cluster analysis (HCA) (Foued et al., 2017). The execution of the multivariate statistical analysis with a large amount of data provides a reliable alternative approach for understanding and interpreting the complex system of water quality (Busico et al., 2018; Yang et al., 2023).

Q-mode cluster analysis is a very useful statistical tool that aims to find relatively homogeneous clusters based on measured features (Ward, 1963). Many researchers have successfully used this technique to classify water samples (Belkhiri et al., 2010a; King et al., 2014; Rafighdoust et al., 2016). In this case, Q-mode cluster analysis is used to classify fresh and thermal waters into different groups based on their physicochemical parameters.

Stable isotopes ^{18}O and ^{2}H are very useful for many hydrogeological studies aimed at studying the source of water in groundwater systems, flow patterns, mixing processes, and the identification of potential evaporative processes (Legrioui et al., 2020). Figure 8 shows the $\delta^{18}O$ and $\delta^{2}H$ for some studied waters where the global meteoric water line GMWL (Rozanski et al. 1993) and the local meteoric water line LMWL (extrapolated by Souag, 1985) are also presented. The types of isotopic analyzes performed are generally composed of stable isotopes.

The current work is an attempt to measure the quality of various water samples from the Tebessa area. This study was conducted to determine the water quality of 23 selected springs and 2 wells in the cities of Hammamet, Tebessa and Morsott, and evaluated the physical and chemical quality of the well and spring samples provided by this study. Analyze to provide detailed information, elucidate the chemical processes responsible for groundwater chemistry, and reconstruct the mechanisms of groundwater formation and recharge. Otherwise, we will assess the groundwater chemistry and quality of the Tebessa Plain and its suitability for drinking and irrigation purposes, and understand the causes and mechanisms that control groundwater chemistry.

Material and methods

Geological and hydrogeology settings

The study area belongs to the Tebessa district and is located at the eastern end of the Saharan Atlas chains, at the Algerian-Tunisian borders, on the northern piedmont of the Nememchats. Lies between the longitudes 7°30' to 8°15' E and the latitudes 35°15' to 35°45' N. It is delimited to the North by Djebel Zitouna, to the South by Djebel Tazbent and Doukkane, to the West by Djebel Matloug and Djebel Mzouzia to the East by Djebel Djebissa and Bouramane (Fig. 1). Many springs emerge in this locality, and thier water contributes to drinking purposes and the irrigation of the communities and farmers of the area.

The study area is characterized by an elevation of about 644 to 1633 m above the sea. Geologically, the study area corresponds to a basin of sedimentation subsiding moderately. It is a tectonic origin pit that is formed during the Tertiary and the Quaternary in which detritus formations of mio-plio-quaternary are accumulated based on a marly substratum to the center of the plain and on the limestone of the Cretaceous to the edges, the Triassic formations appear in the vicinity of Jebel Djebissa and Jebel Belkfif. Triassic pointings are also observed at Jebel Hameimat as well as a Triassic outcrop is reported around Youkous the baths in Hammamet (Fig. 1). The geometry of the Mio-Plio-Quaternary reservoir depends on the nature of sediment deposits that passes 500 m of thickness in the center of the plain The Tebessa region is characterized by anticlinal and synclinal structures of NE-SW orientation, resulting from the pre-Miocene folding phase, affecting the Cretaceous formations (Blés & Fleury, 1970; Vila, 1980). The aquifers are mainly recharged by precipitation; secondarily the infiltration of water from faults (cretaceous formation) is another possible source of aquifer recharge. The climate of the study area is considered to be semi-arid, with a very hot and dry summer and very cold and wet winter. The precipitation average is between 350 and 400 mm. The temperature can rise in the summer to 40 °C. This situation of dryness accentuates the drawdown of water resources, especially during the last decade, because the

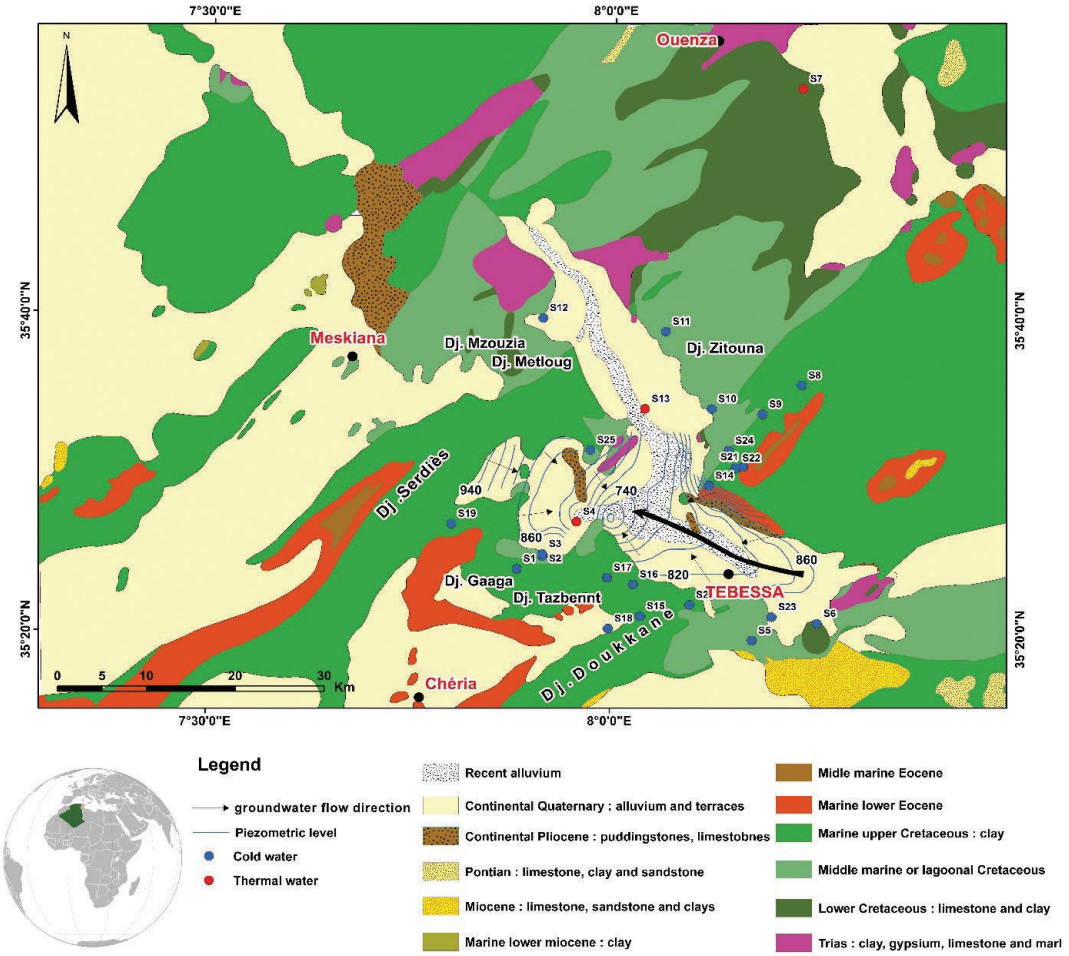

Fig. 1 - Study area geological map.

Fig. 1 - Carta geologica dell'area di studio

renewal of this resource is very weak. Vegetation consists of forests, maquis, and reforestation the remaining area is divided between agricultural and wastelands. The development of agriculture is strongly influenced by soil properties, runoff, and the intensity of human activities.

Water sampling and analysis

Twenty-five water samples were collected during the month of April 2018 in the Tebessa area (Fig. 1). The physical parameters such as pH, temperature (°C), Electrical Conductivity (EC), and Total Dissolved Solids (TDS) were measured in-situ using a portable conductivity meter (HANNA Hi-9813-6 Multiparameter). All samples were kept at a temperature of less than 4 °C in a refrigerator until further analyses (within 1 week) in the laboratory of the National Hydraulic Resources Agency (ANRH) in Constantine. Chemical parameters of groundwater samples, such as the main cations, calcium (Ca^{2+}) and magnesium (Mg^{2+}) were determined using the EDTA titration method. Sodium (Na^{+}) and potassium (K^{+}) were measured by frame photometry. Anions such as bicarbonate (HCO_3^{-}) were determined by titration to the methyl orange endpoint. The amount of chloride (Cl^{-}) present in groundwater samples was determined by titration and precipitation of AgCl against the appearance of silver chromate. Sulfate (SO_4^{2-}) was determined by precipitating $BaSO_4$ and measuring absorbance with a spectrophotometer. Organic substances such as nitrates (NO_3^{-}) were measured by the phenoldisulfonic acid method.

Statistical analysis

Principal Component Analysis (PCA) is one of the unsupervised linear techniques in multivariate data analysis. This technique was generally used to identify parameters and pollutant sources (Bouaicha et al., 2019; Kassahun & Kebedee, 2012). It is performed to reduce a large data set of variables into a few new linear uncorrelated (i.e. orthogonal) variables factors called principal components (PCs) (Farnham et al., 2003; Wold et al., 1987). PCs are also called latent variables. These factors can be interpreted to reveal the underlying data structure. The first principal component (PC1) accounts for the maximum possible proportion of the total variance in the

data set, and the second component (PC2) accounts for the maximum of the remaining variance, and so on. The maximum number of PCs is equal to the number of variables. The total variance accounted for by all the PCs will be equal to the number of variables. For interpretation, only a few of PCs are retained in the analysis. PCA can be explained by scores and loading plots. The scores plot explains the relations between samples, and the loading plot explains the relationships between variables (Xanthopoulos et al., 2013).

Cluster analysis is a branch of multivariate techniques whose primary purpose is to cluster objects based on the properties they possess. According to predetermined selection criteria, cluster analysis divides objects into a few clusters so that objects in the same group have the most similar characteristics (Valder et al., 2012).

HCA Q-mode is the most widely used cluster analysis technique in hydrogeology (Ayenew et al., 2009a; Belkhiri et al., 2010b; King et al., 2014b; Rafighdoust et al., 2016a; Bouteraa et al., 2019), and it can identify the initial relationship between any sample and the entire dataset, typically visually illustrating the relationship with a dendrogram (Ayenew et al., 2009b; Shrestha & Kazama, 2007). In this study, HCA was performed on standardized hydrochemistry datasets using Ward's linkage rule (Ward, 1963), which generates different groups based on an analysis of variance and then groups all non-residuals into separate clusters. Each sample in a cluster is more similar to the other samples in the same cluster than to samples in other clusters. The Euclidean distance is used in HCA as a measure of similarity between all samples (Raiber et al., 2012b).

The interpretation and integration of the obtained data using different geochemical ratios and the most common representations are obtained by the use of XLSTAT® (Demo version 2021), PhreeqC 3.0.6, and Originlab® 2021.

Water Quality Index (WQI)

The water quality index is a numerical expression designed to determine the ecological status of a water body. For the general calculation of this index, it is generally necessary to determine the physical, chemical, and biological parameters (Akhtar et al., 2021; Amadi, 2011; Gebrehiwot et al., 2011). This method generally does not limit the calculation of all physical and chemical parameters and biological parameters at the same time, and can also be calculated separately. When using this method, it is very important to consider changes in physical and chemical parameters, which are mainly due to human factors, but there are also natural processes such as hydrology, topography, and lithology. According to the calculated value of the WQI index, the water samples to be inspected can be classified into one of the following water quality categories: excellent, good, poor, very poor or, undrinkable (Goher et al., 2015; Mahapatra et al., 2012; Paiu Mădălina & Breabăn Iuliana Gabriela, 2014; Shweta, 2013). The water quality data are recorded and transferred to a weighting curve chart, where a numerical value of Qi is obtained. The mathematical expression for WQI is given by the following equation:

$$WQI = \frac{\sum QiWi}{\sum Wi} \quad (1)$$

The quality rating scale (Qi) for each parameter is calculated by using this expression:

$$Qi = 100\left[\left(\frac{Vi - Vo}{Si - Vo}\right)\right] \quad (2)$$

Where Vi is the estimated concentration of the parameter in the analyzed water.

Vo is the ideal value of this parameter in pure water. Vo = 0 (except pH =7.0)

Si is recommended standard value of the parameter

Unit weight was calculated by a value inversely proportional to the recommended standard value Si of the corresponding parameter

The unit weight (Wi) for each water quality parameter is calculated by using the following formula:

$$Wi = \frac{K}{Si} \quad (3)$$

Where K = proportionality constant and can also be calculated by using the following equation:

$$K = \frac{1}{\sum(1/Si)} \quad (4)$$

The rating of water quality according to this WQI is given in Table 1.

Tab. 1 - Water Quality Rating as per Weight Arithmetic Water Quality Index Method.
Tab. 1 - Classificazione della qualità delle acque per il Weight Arithmetic Water Quality Index Method.

Water Quality Water Value	Rating of Water Quality
0-25	Excellent Water Quality
26-50	Good Water Quality
51-75	Moderate Water Quality
76-100	Poor Water Quality
>100	Unsuitable for Drinking

Geochemical modeling

The saturation index (SI) is a widely used indicator in the hydrogeochemical studies. It describes the saturation status of minerals in the groundwater. On equilibrium conditions of the solution concerning a given mineral. It is defined by the following equation:

$$SI = \log(Kiap/Ksp) \quad (5)$$

Where: Kiap is the ion activity product, and Ksp is the equilibrium constant. When Kiap = Ksp, the SI value is 0 and the aqueous solution is at equilibrium regarding the given mineral. If SI > 0, the solution is supersaturated with the components of the considered mineral. If SI < 0, the solution is undersaturated with respect to the mineral. The hydrogeochemical modeling code, PHREEQ-C was used to calculate the SI (Appelo et al., 1990; Parkhurst & Appelo, 1999 a, b).

Results and discussion

Statistical analysis

The output of the Q-mode cluster analysis is given as a dendrogram (Fig. 2). Two preliminary groups are selected based on a visual examination of the dendrogram, each representing a hydrochemical facies (Table 2).

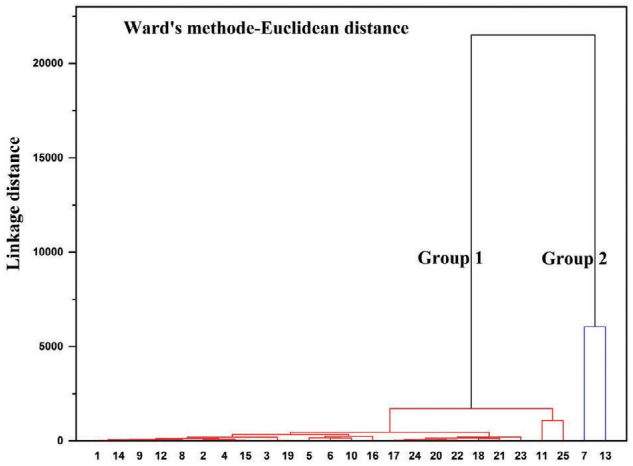

Fig. 2 - Dendrogram of the hydrochemical samples.

Fig. 2 - Dendrogramma della composizione chimica dei campioni.

The first water group, **Group 1**, has low salinity (mean EC = 644 µS/cm) and abundance orders (mg/L) Ca^{2+} > Mg^{2+} > Na^{+} > K^{+} and HCO_3^{-} > Cl^{-} > SO_4^{2-} > NO_3^{-} (Fig. 3). The average water temperature was 15.16°C. This water is classified as an HCO_3^{-} alkaline earth water type. It consists of water samples where the cation composition is dominated by Ca^{2+} and Mg^{2+} and the anion composition varies from predominantly HCO_3^{-} to predominantly Cl^{-} and SO_4^{2-} (Fig. 3). **Group 2**, consisting of two water samples, shows a high salinity range (18050 > EC > 23700 µS/cm; mean value 20850 µS/cm). Based on overall chemical composition, characterized by ion abundances Na^{+} > Ca^{2+} > Mg^{2+} > K^{+} and Cl^{-} > SO_4^{2-} > HCO_3^{-} > NO_3^{-}, these waters are classified as Na^{+}- Cl^{-} types (Fig. 2). The most pronounced characteristic of this group is the increase in the Cl^{-} and Na^{+} content. Their temperatures vary between 25 and 37 °C.

Tab. 2 - Mean parameter values of the two principal water groups.

Tab. 2 - Valori medi dei parametri dei due principali gruppi di acque.

Chemical parameter	Group	
	I	II
EC (µS/cm)	554.77	20875
TDS	428.95	12671.5
pH	7.43	6.41
T (°C)	15.93	31
Ca^{2+} (mg/L)	75.98	1308.8
Mg^{2+} (mg/L)	24.46	136.28
Na^{+} (mg/L)	28.29	3060
K^{+} (mg/L)	0.8	18
HCO_3^{-} (mg/L)	221.27	1137.65
Cl^{-} (mg/L)	39.83	6500
SO_4^{2-} (mg/L)	84.74	506
NO_3^{-} (mg/L)	17.04	5

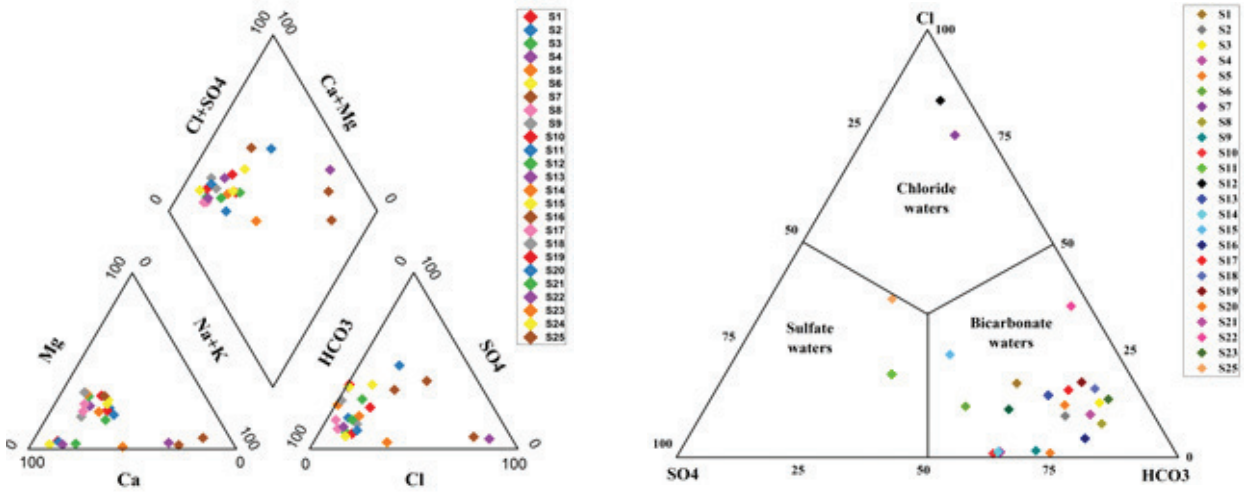

Fig. 3 - Piper and Cl–SO4–HCO3 ternary diagram.

Fig. 3 - Diagramma di Piper e diagramma ternario Cl–SO_4–HCO_3

Tab. 3 - Pearson's correlation coefficients between physicochemical parameters for groundwater samples.

Tab. 3 - Coefficienti di correlazione di Pearson tra i parametri fisico-chimici dei campioni di acqua.

	Ca^{2+}	Mg^{2+}	Na^{+}	K^{+}	HCO_3^{-}	Cl^{-}	SO_4^{2-}	NO_3^{-}	T	EC	pH
Ca^{2+}	1										
Mg^{2+}	0.88	1									
Na^{+}	**0.99**	**0.86**	1								
K^{+}	0.65	0.49	0.74	1							
HCO_3^{-}	0.90	**0.75**	**0.94**	**0.87**	1						
Cl^{-}	**0.99**	**0.87**	**0.996**	0.70	**0.92**	1					
SO_4^{2-}	0.74	**0.81**	0.78	0.65	0.77	0.75	1				
NO_3^{-}	-0.18	0.09	-0.16	-0.05	-0.16	-0.18	0.23	1			
T	**0.61**	0.49	0.65	**0.71**	0.74	0.63	0.56	-0.23	1		
EC	**0.99**	**0.89**	**0.997**	**0.71**	**0.93**	**0.998**	**0.78**	-0.14	**0.64**	1	
pH	**-0.54**	-0.64	-0.54	**-0.51**	**-0.62**	-0.54	-0.60	-0.02	-0.63	-0.56	1
Bold values represent the strong correlations between physicochemical and chemical characteristics											

In this study, PCA was applied to the hydrochemical parameters of the 25 thermo-mineral waters analyzed (Table 3). The first three factors, F1, F2, and F3, represent 90.1% of the total variance. Factor 1 (71.04%) has a strong loading of EC, HCO_3^{-}, Cl^{-}, Ca^{2+}, and Na^{+} (Table 4). It is defined as the salinity factor since it reflects the different sources of groundwater salinization: the dissolution of evaporate minerals, and HCO_3^{-} shows a strong positive loading on this axis as explained by the dissolution/precipitation of carbonate minerals. The second factor explains 11.28% of the total variance. A likely explanation for the positive correlation observed with nitrate is its association with agricultural practices, specifically the use of fertilizers. Factor 3 exhibits 7.76 % of the total variance. It shows a high positive loading on temperature, which explains the role of geothermal manifestations.

Tab. 4 - Variables-factors correlation.

Tab. 4 - Valori di correlazione di ciascuna variabile nei fattori individuati.

	F1	F2	F3
Ca^{2+} (mg/L)	**0.956**	-0.079	-0.260
Mg^{2+} (mg/L)	**0.877**	0.257	-0.257
Na^{+} (mg/L)	**0.976**	-0.067	-0.182
K^{+} (mg/L)	0.794	-0.055	0.362
HCO_3^{-} (mg/L)	**0.962**	-0.095	0.081
Cl^{-} (mg/L)	**0.965**	-0.088	-0.228
SO_4^{2-} (mg/L)	**0.840**	0.386	0.032
NO_3^{-} (mg/L)	-0105	**0.958**	0.056
T (°C)	0.746	-0.218	**0.508**
EC (µS/cm)	**0.976**	-0.044	-0.201
pH	-0.682	-0.172	-0.443
Eigenvalue	7.815	1.242	0.854
Variance (%)	71.044	11.287	7.763
Cumulative variance (%)	71.044	82.332	90.095
Bold values indicate significant loading of water parameter			

Factors F1, F2, and F3 reflect the main factors that control the geochemistry of groundwater, which is: the dissolution of evaporate minerals (halite and gypsum), ion exchange of Ca^{2+} (and/or Mg^{2+}) by Na^{+}, and dissolution/precipitation of carbonate minerals. In consistency with obtained data from the geochemical characterization of the sampled waters, the multivariate analyses indicate that marl and gypsum dissolution largely contribute to groundwater mineralization. The evaporitic chloride-sulfate minerals represent an additional source of groundwater salinity.

Hydrogeochemical process

For samples of thermo-mineral water from Tebessa, Piper diagram (Piper, 1944) and ternary diagram Cl^{-} - SO_4^{2-} - HCO_3^{-} (Fig. 3), show that the thermal springs of the Tebessa region are characterized by the predominance of bicarbonate in relation to carbonate, and cations are mainly represented by calcium. The main types of groundwater Ca^{2+}- HCO_3^{-}, and Na^{+} - SO_4^{2-} can be explained by leaching the Triassic layer in the study area. To determine the possibility Group of water by physical and chemical composition, the statistical analysis of the chemical elements of the spring water samples is reported in Table 5. According to the analytical data, all the spring water samples investigated can be classified into two groups.

Group 1, by far the most important one is representative of most freshwater springs which emerge from carbonate aquifer (cretaceous limestones) (Fig. 1). The first group of waters samples is low in mineralization. Thus only a few springs indicate high concentrations exceeding the norm, as is the case of S11 in the south of Morsott city, and S25 in Bir D'hab. Most of these concentrations are related to the dissolution of Triassic formations of Djebel Belekfif. Among the major cations Table 5, a predominance of Ca^{2+} followed by Mg^{2+}, Na^{+}, and K^{+} is observed for the first group of freshwater springs, Concentrations of both Ca^{2+} and Mg^{2+}(in mg/L) represent on average 54 and 26% of all the cations, respectively. Na^{+}- K^{+}

Tab. 5 - Hydrochemical summary of the springs.

Tab. 5 - Sintesi della composizione idrochimica delle sorgenti.

ID	Spring	TDS	EC (µS/cm)	pH	T (°C)	Ca^{2+} (mg/L)	Mg^{2+} (mg/L)	Na^{+} (mg/L)	K^{+} (mg/L)	HCO_3^{-} (mg/L)	Cl^{-} (mg/L)	SO_4^{2-} (mg/L)	NO_3^{-} (mg/L)
S1	Aïn Gaâgaâ	408	570	7.31	15	51.52	31.44	20	0.8	170.8	50	68	15
S2	Aïn Ammacha	502	680	7.06	14.5	62.69	29.64	34	1	262.3	35	64	13
S3	Youkous	321	430	7.48	14	42.3	22.56	10	0.7	183	30	22	10
S4	Hammamet	528	660	6.72	35	72.8	30.68	21	0.8	256.2	5	140	2
S5	Aïn T'noukla	635	800	6.86	15	85.77	48.22	18	0.8	353.8	5	120	3
S6	Aïn El Khangua	713	880	7.03	15	87.2	50.88	43	2	237.9	55	168	70
S7	Sidi Yahia El Madani	11242	18050	6.32	37	1046.2	89.86	2770	30	1299.3	5500	500	7
S8	Guastel	465	580	7.89	15	63.15	26.88	14	1	256.2	25	36	43
S9	Aïn El Hadj	455	530	7.3	16	68	19.21	15	2	225.7	5	88	32
S10	Aïn Chamla	821	940	6.88	16	89.19	38.11	46	1	353.8	5	206	12
S11	Aïn El Hedjar	1152	1640	7.14	16	159.44	63	101	1	256.2	150	366	55
S12	Aïn Sidi Khaled	438	520	7.4	16	63.8	19.36	33	0.8	189.1	35	88	9
S13	Forage ST	14101	23700	6.5	25	1571.4	182.7	3350	6	976	7500	512	3
S14	Aïn Kissa	456	590	7.21	15	64.01	24.40	26	1	207.4	45	58	30
S15	Aïn Tebinet	516	610	7.24	15	62.64	32.64	30	2	237.9	5	132	14
S16	Ain Sari	412	876	7.5	14	76.1	47.5	32.2	1.9	99	56	78.1	21.5
S17	A El Annba	334	120	7.5	15	52.07	17.8	12.8	0.2	197	11	40.8	2.1
S18	Lemgalibe	186	254	8	14	28.04	15.9	5.3	0.1	95	21.3	19	10.9
S19	Troubia	354	415	7.4	15	78.06	4.3	11	0.2	175	37.3	20	21.9
S20	Mizeb	359	190	72	15	76.8	3.76	11.5	0.1	191.50	46.8	27.9	1
S21	Ain Kababcha	140	291	8.3	15	84	3.36	23.59	0.1	206.76	35.5	48	0.5
S22	Ain Kebira	95	196	7.2	16	104	3.24	19.22	0.1	246.66	31.95	40	2
S23	Ain Salhi	60	294	8.3	14	104	2.4	86.25	0	259.86	150.8	15.84	3.41
S24	Ain Zouigha	30	129	7.90	15	96.00	2.88	9.56	0.1	206.76	35.5	18.72	3.55
S25	Fedha	1781	2610	7.52	15	75.93	37.5	472	4	280.6	425	442	44

Acque Sotterranee - *Italian Journal of Groundwater* 2023-AS45-667: 77 - 90

DOI 10.7343/as-2023-667

ions are secondary in importance, representing on average 19% of all cations. Among the major anions, HCO_3^- generally dominates, representing on average 55% of all the anions followed by SO_4^{2-}, however, the NO_3^- indicates that several springs contain groundwater with insignificant amounts of NO_3^- (Table 5). Cl^- is less abundant; they represent on average 18% of all the anions, respectively. In contrast to this, the predominant anion trend is in the order HCO_3^-> SO_4^{2-} > Cl^- > NO_3^- in the spring S5 and S8 and in cations, the order is Ca^{2+} > Mg^{2+} > Na^+ > K^+.

Group 2, the second group involves especially the thermal springs (hot water springs) from the Triassic formations, is formed by three springs (S4, S7, and S13) and show relatively high total dissolved solids (TDS) contents, with values ranging from 528 to 14101 mg/L, the average value being 8623.67 mg/L. The temperature of the thermal water samples varies from 25 to 37°C. The EC values of the samples vary from 680 to 23700 µS/cm and the pH values range from 6.32 to 6.72 (Table 5), indicating strongly mineralized and acidic waters (relation with Triassic rocks). The order of abundance of the major ions is Na^+ > Ca^{2+} > Mg^{2+} > K^+ and Cl^- > HCO_3^- > SO_4^{2-} > NO_3^-, and the hydrochemical type is characterized by Na^+ - Cl^- facies (S7 and S13). It is linked to clay formations, evaporates, and the presence of the Triassic (Djebel Belkfif, el Meridj city). On the other hand the thermal spring of H. Salihine (S4) which presents low mineralization localized in El Hammamet city. The order of abundance of the major ions is Ca^{2+} > Mg^{2+} > Na^+ > K^+ and HCO_3^- > SO_4^{2-} > Cl^- > NO_3^-, and the hydrochemical type is characterized by Ca^{2+} - HCO_3^- facies (S4), suggesting that this sample water is mainly influenced by deep carbonate reservoir rocks.

The Piper diagram showed a remarkable dominance of calcium bicarbonate facies in the 21 springs (Fig. 3), known by the presence of abundant carbonate outcrops of the plain (Maastrichtian limestone), but the facies in S7, S13, and S25 sources are sodium chloride, explained by the dissolution of evaporate minerals (the leaching of Triassic marls). In addition, the facies in S11 is calcium sulfate, it is positively correlated with nitrates and linked to agricultural activity, which is due to the use of fertilizers.

Water-interaction in the aquifer the different compositions of groundwater types result from several hydrochemical processes. Interactions between groundwater and host rocks are the main processes controlling the chemical characteristics of groundwater in the studied area. Calcium and magnesium in groundwater result from the leaching of limestone, dolomites, and gypsum, as well as from the cation exchange process. The reaction of carbonate minerals (calcite and dolomite) with water and carbon dioxide can be expressed with the following equation:

$$CaCO_3\ (calcite) + H_2O + CO_2 \rightarrow Ca^{2+} + 2HCO_3^- \quad (6)$$

$$CaMg(CO_3)_2\ (dolomite) + 2H_2O + 2CO_2 \rightarrow Ca^{2+} + Mg^{2+} + 4HCO_3^- \quad (7)$$

Plot (Ca^{2+} + Mg^{2+}) versus (HCO_3^-) (Fig. 4a) shows that the majority of samples are clustered close to the 1:1 line and represent an excess HCO_3^- over (Ca^{2+} + Mg^{2+}), suggesting an additional source of carbonate minerals (calcite and dolomite) rather than Ca^{2+} and Mg^{2+}. The plot (Ca^{2+} + Mg^{2+}) versus (HCO_3^- + SO_4^{2-}) (Fig. 4c) shows that most of the samples cluster around the 1:1 line, indicating that the dissolutions of calcite, dolomite, and gypsum are the dominating processes in the system, as shown in the Eqs. (6), (7), and (8). The Na^+-Cl^- relationship has often been used to identify the mechanisms for acquiring salinity in semi-arid regions (Dixon & Chiswell, 1992b; Magaritz et al., 1981a). The Na^+ and Cl^- contents high detected in certain samples may suggest the dissolution of chloride salts. The dissolution of halite in water releases equal concentrations of Na^+ and Cl^- into the solution:

$$CaSO_4.\ 2H_2O \rightarrow Ca^{2+} + SO_4^{2-} + 2H_2O \quad (8)$$

$$NaCl \rightarrow Na^+ + Cl^- \quad (9)$$

Dissolution of some ions indicates a re-concentration process by dissolution or evaporation of the chloride salt. Figure 4d shows the Cl^- value as a function of Na in a groundwater sample and there is a strong correlation between the two (r = 0.99). However, some of the samples in Figure d deviate from the expected 1:1 ratio, indicating that some of the Na must be derived from other processes.

The plot of Ca^{2+} + Mg^{2+} vs. Cl^- (Fig. 4b) indicates that Ca^{2+} and Mg^{2+} increase with increasing salinity. This may be due to reverse ion exchange in the clay/weathered layer. During this process, the aquifer matrix may adsorb dissolved sodium in exchange for bound Ca^{2+} and Mg^{2+}.

Geochemical modeling

The outcomes of the saturation index calculations for specific minerals examined (calcite, aragonite, dolomite, gypsum, anhydrite, and halite) are shown in Table 6. As a result, most groundwater samples are in an undersaturation state with halite, gypsum, and anhydrite minerals (SI<0), as seen in Figure 5, the analyzed waters are plotted largely below the equilibrium state with SI gypsum, SI anhydrite, and SI halite ranging respectively from -0.50 and -2.63, -0.77 and -3.06, and -8.68 to -3.37. The chemical composition of groundwater is partially controlled by mineral dissolution, from evaporate (halite, gypsum, and anhydrite) and carbonate minerals. However, in the case of oversaturation (SI>0) with respect to carbonate minerals (calcite, dolomite and aragonite) ranges both between -1 and 1 for the majority of water samples (Hamad et al., 2018).

Hydrogeochemical evolutionary methods proposed by others are used to test mineral stability diagram. (Barkat et al., 2021; Bouteraa et al., 2019; Foued et al., 2017; Güler & Thyne, 2004). Activity plots of log(aCa^{2+}/$a2H^+$) vs log(aNa^+/aK^+), log(aCa^{2+}/$a2H^+$) vs log(aMg^{2+}/$a2H^+$), and log(aMg^{2+}/$a2H^+$) vs log(aNa^+/aK^+) were obtained for the four mineral Indicates stability. 25 °C, at 1 bar. The two water groups are essentially plotted in the Ca smectite and kaolinite stability fields. Therefore, the balance between Ca smectite and kaolinite is one of the major processes regulating the chemical composition of water in the study area (Barkat et al., 2022;

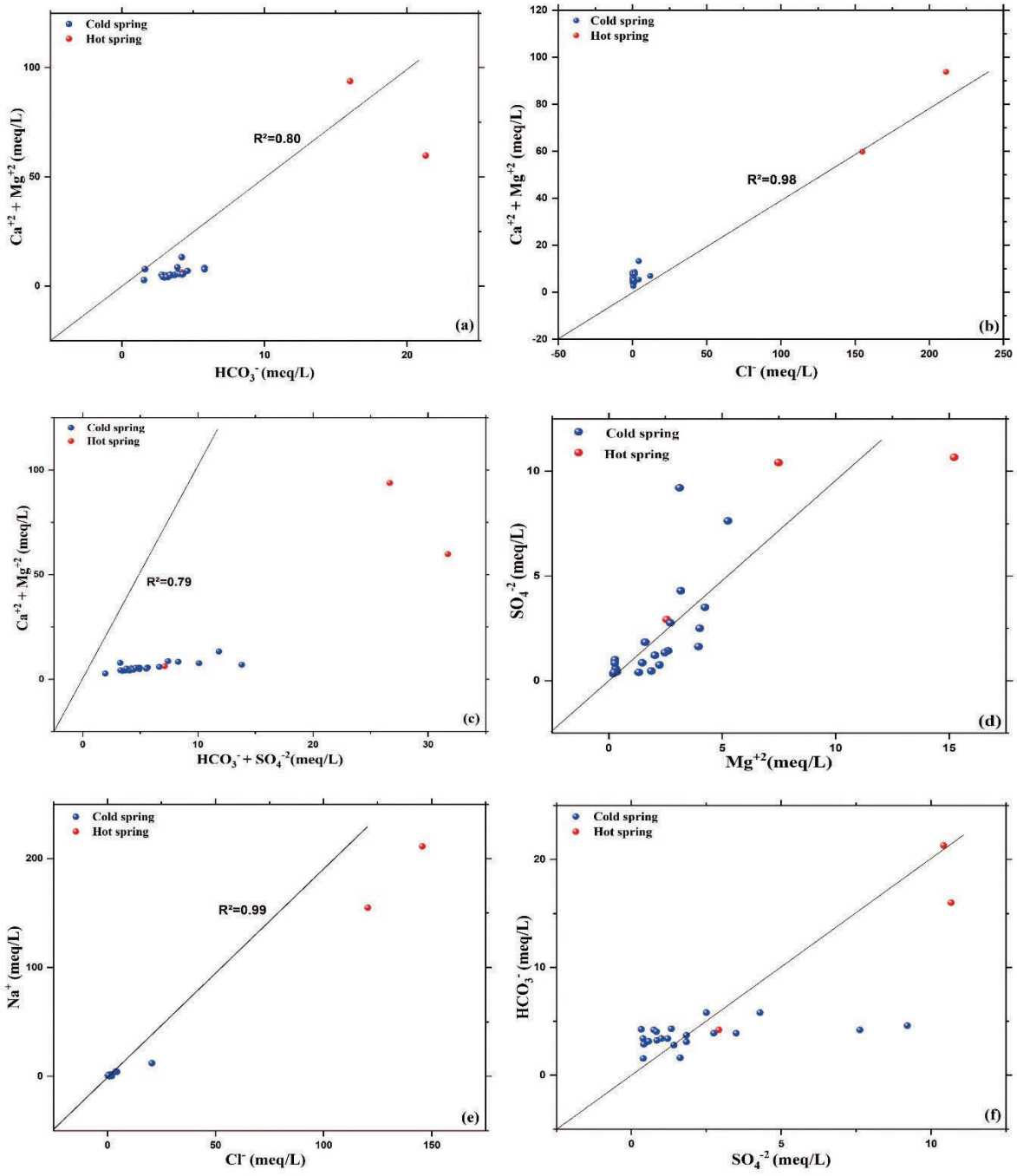

Fig. 4 - Bivariate plots (a) Ca^{2+} + Mg^{2+} versus HCO_3^-; (b) Ca^{2+} + Mg^{2+} versus Cl^-; (c) Ca^{2+} + Mg^{2+} versus HCO_3^-+SO_4^{2-}; (d) Mg^{2+} versus SO_4^{2-}; (e) Na^+ versus Cl^-; and (f) HCO_3^- versus SO_4^{2-}.

Fig. 4 - Diagrammi bivariati: (a) Ca^{2+} + Mg^{2+} vs HCO_3^-, (b) Ca^{2+} + Mg^{2+} vs Cl^-, (c) Ca^{2+} + Mg^{2+} vs HCO_3^-+SO_4^{2-}, (d) Mg^{2+} vs SO_4^{2-}, (e) Na^+ vs Cl^-, and (f) HCO_3^- vs SO_4^{2-}.

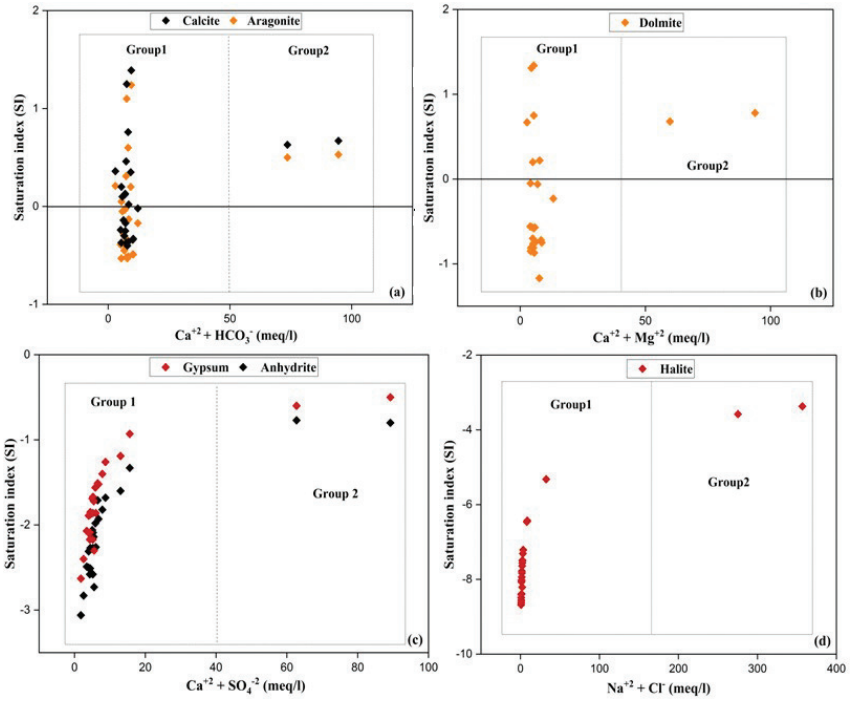

Fig. 5 - Saturation index of a) Calcite–Aragonite, b) Dolomite, c) Gypsum–Anhydrite, and d) Halite.

Fig. 5 - Indice di saturazione di a) Calcite–Aragonite, b) Dolomite, c) Gesso –Anidride, and d) Halite.

Tab. 6 - Saturation indices of groundwater samples.

Tab. 6 - Indici di saturazione dei campioni di acqua sotterranea.

	IS anhydrite	IS aragonite	IS calcite	IS dolomite	IS gypsum	IS halite
S1	-2.31	-0.53	-0.37	-0.76	-1.89	-7.56
S2	-2.27	-0.52	-0.37	-0.87	-1.85	-7.49
S3	-2.83	-0.39	-0.24	-0.56	-2.40	-8.07
S4	-1.71	-0.53	-0.40	-0.74	-1.51	-8.56
S5	-1.93	-0.49	-0.34	-0.72	-1.52	-8.62
S6	-1.82	-0.51	-0.36	-0.75	-1.40	-7.21
S7	-0.77	0.50	0.63	0.68	-0.60	-3.58
S8	-2.50	0.31	0.46	0.75	-2.09	-8.02
S9	-2.09	-0.32	-0.17	-0.70	-1.67	-8.68
S10	-1.68	-0.49	-0.33	-1.17	-1.26	-8.21
S11	-1.33	-0.17	-0.02	-0.23	-0.93	-6.43
S12	-2.06	-0.29	-0.14	-0.57	-1.69	-7.50
S13	-0.80	0.53	0.67	0.78	-0.50	-3.37
S14	-2.29	-0.45	-0.30	-0.81	-1.88	-7.49
S15	-1.98	-0.40	-0.25	-0.57	-1.56	-8.39
S16	-2.14	0.05	0.20	0.22	-1.72	-7.31
S17	-2.49	-0.05	0.10	-0.05	-2.07	-8.40
S18	-3.06	0.21	0.36	0.67	-2.63	-8.49
S19	-2.58	-0.03	0.12	-0.81	-2.17	-7.94
S20	-2.51	-0.03	0.13	-0.85	-2.09	-7.83
S21	-2.27	1.10	1.25	1.31	-1.86	-7.64
S22	-2.26	0.20	0.35	-0.58	-1.86	-7.78
S23	-2.73	1.24	1.39	1.34	-2.30	-6.46
S24	-2.58	0.60	0.76	0.20	-2.17	-8.03
S25	-1.60	-0.13	0.02	-0.06	-1.19	-5.32

Bouteraa et al., 2019). As a result, the main geochemical reaction that controls the chemistry of the underground waters of the Tebessa Plain can be written as:

$$6CaAl_2\,SiO_{10}\,(OH)_2 + 2H^+ + 23H_2O \leftrightarrow 7Al_2Si_2O_5\,(OH)_4 + Ca^{2+} + 8H_4SiO_4a^2 + 8H4SiO_4 \quad (9)$$

(Ca – Smectite) (Kaolinite)

$$MgAl_2SiO_{10}\,(OH)_2 + 2H^+ + 23H_2O \leftrightarrow 7Al_2Si_2O_5\,(OH)_4 + Mg^{2+} + 8H4SiO_4$$

(Mg – Smectite) (Kaolinite)

Mineral stability diagrams are first used to identify the reactions that mechanism the chemistry of water. Figure 6 reveals mineral stability fields for a weathering kaolinite system (Na_2O–Al_2O_3–SiO_2–H_2O), indicating that equilibrium with this mineral phase is one of the main processes controlling groundwater chemistry.

Isotopic geochemistry

Hydrochemical and isotope analyses were used to study the chemical processes responsible for groundwater chemistry and reconstruction of the origin and groundwater recharge mechanisms in recent years. Previous studies showed that the study area is influenced by both the Atlantic Ocean and the southern Mediterranean Sea precipitations (Gayar & Hamed, 2018; Hamad et al., 2018). The types of isotopic analyses performed are generally composed of stable isotopes (oxygen 18 and deuterium).

The main cold springs of the study area have been studied by means of stable isotope measurements (Fig. 7), ^{18}O values for spring and well samples varies between -8.62 and -5.46

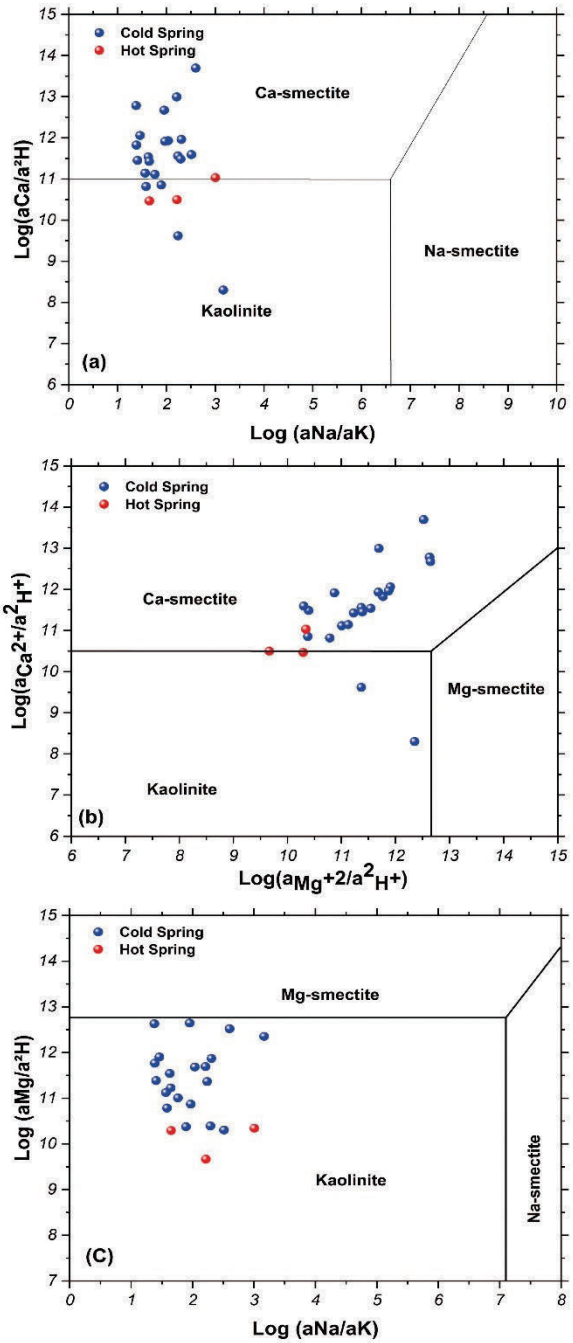

Fig. 6 - Mineral stability diagrams.

Fig. 6 - Diagrammi di stabilità dei minerali.

‰, for the same time ^{2}H values range from -64.62 to -30.28 ‰ (Table 7). According to the diagram $\delta^{18}O/\delta^{2}H$ (Fig. 7), the water springs are plotted together with the Local Meteoric Waterline (LMWL) and the Global Meteoric Waterline (GMWL), water springs show two different groups. **Group 1** indicates no significant isotopic modifications by evaporation. It refers to the majority of Maastrichtian samples located generally above the LMWL and presenting an enrichment of both heavy isotopes, whereas the Cenomanian and Eocene water samples are plotted below the two meteoric water lines

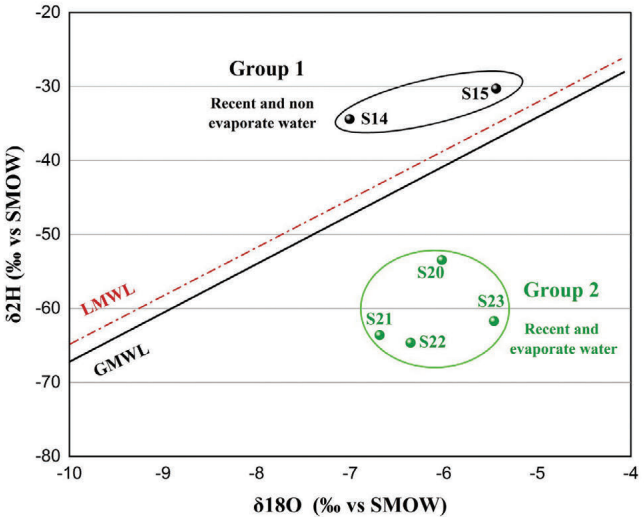

Fig. 7 - Relationship of ^{18}O and ^{2}H related to the global meteoric water line and Mediterranean water line.

Fig. 7 - Relazione tra ^{18}O e ^{2}H con la retta meteorica globale e la retta meteorica mediterranea.

Tab. 7 - Results of isotopic (^{18}O and ^{2}H) analyses of Tebessa region.

Tab. 7 - Risultati delle analisi isotopiche (^{18}O e ^{2}H) della regione di Tebessa.

Sample	Name	Hydrogeological unit	Altitude (m)	$\delta^{18}O$ ‰	$\delta^{2}H$ ‰
S14	Ain Kissa	Maastrichtian	1000	-7.0061	-34.4090
S15	Ain Ksar Tebinet	Maastrichtian	1380	-5.4401	-30.2880
S20	Ain El Mizeb	Turonien	1070	-6.0196	-53.4451
S21	Ain Kababcha	Eocène	1300	-6.6854	-63.6028
S22	Ain Kabira	Eocène	1280	-6.3549	-64.6294
S23	Ain Salhi	Albien	940	-5.4628	-61.6958

composing **Group 2**, characterized by intense evaporation of the rainfall water during infiltration in carbonate fractures. Isotopic analysis from the Tebessa region indicates that groundwater from the karst aquifer is of meteoric origin (Chabour et al., 2021; Hamad, Baali et al., 2018; Kouadra et al., 2019; Legrioui et al., 2020). This must therefore be rapid, taking place through a fissure and/or karst network.

Water quality index

One of the advantages of using a water quality index in assessing the overall quality of water is that it sums up numerous data points into a single value in an impartial, rapid, and logical way. Furthermore, it evaluates different areas and detects changes in water quality, and an index value can relate to the potential use of that water (Mishra, 2010; Tyagi et al., 2020). For the study area, the WQI value is designed for drinking water using the guidelines established by (WHO, 2011). The values of WQI are presented in Table 8.

Tab. 8 - Suitability of groundwater for drinking based on WQI.

Tab. 8 - Utilizzabilità dell'acqua sotterranea per scopo potabile basata sul WQI.

WQI Level	Class	Sample number	% of samples
0-25	Excellent Water Quality	S2, S4, S5, S10, S20, S22	24%
26-50	Good Water Quality	S1,S3,S6,S8,S9,S11,S12,S14,S15,S16,S17,S18,S19,S21,S24	60%
51-75	Moderate Water Quality	S23, S25	8%
76-100	Poor Water Quality	Nil	-
> 100	Unsuitable for Drinking	S7, S13	8%

Conclusion

Generally, the groundwater in the study area is dominated by calcium and bicarbonate ions. Ca^{2+} - HCO_3^- and Ca^{2+} - Mg^{2+} - HCO_3^- are the dominant hydrochemical facies with low salinity concentrations present in the study area. However, a Na^+ - Cl^- facies with high mineralization, characterizes the thermal springs. The chemical composition of the water is influenced by the dissolution and/or precipitation processes during the water rock interaction and by the cationic exchange reactions between groundwater and carbonate formations with regard to fresh springs and between groundwater and evaporate formations as for thermal springs. The increasing salinity of these hot waters (S7 and S13) makes them unsuitable for both domestic consumption and agriculture activities.

Thus, hydrogeochemical processes that control groundwater chemistry were identified. This leads to an improved understanding of the hydrogeochemical characteristics of the aquifer. The isotopic analysis of some groundwater samples shows a similarity with the meteoric waters, which reflects their short residence time and low evaporation of the infiltrated water.

Acknowledgments

The authors are thankful to the ANRH administration to provide the necessary analyses to complete this work. The authors wish to give special thanks to Doc. Omar Hamad of Tebessa University, Department of Earth Sciences, for necessary help.

Funding source

This work was self-funded by the authors.

Competing interest

The authors declare no competing interest.

Author contributions

All authors: Yacine LEKRINE, Abdeslam DEMDOUM, Foued BOUAICHA contributed to the data collection, data processing, results interpretation, writing, review, study conception and design.

All authors read and approved the final manuscript.

Additional information

Supplementary information is available for this paper at https://doi.org/10.7343/as-2023-667

Reprint and permission information are available writing to acquesotterranee@anipapozzi.it

Publisher's note Associazione Acque Sotterranee remains neutral with regard to jurisdictional claims in published maps and institutional affiliations.

REFERENCES

Akhtar, N., Ishak, M.I.S., Ahmad, M.I., Umar, K., Md Yusuff, M.S., Anees, M.T., Qadir, A., & Ali Almanasir, Y.K. (2021). Modification of the Water Quality Index (WQI) Process for Simple Calculation Using the Multi-Criteria Decision-Making (MCDM) Method: A Review. Water, 13(7), 905. https://doi.org/10.3390/w13070905

Amadi, A.N. (2011). Assessing the effects of Aladimma dumpsite on soil and groundwater using water quality index and factor analysis. Australian Journal of Basic and Applied Sciences, 5(11), 763–770.

Appelo, C., & Williemsen, A. Beekmanhe Grippioen (1999) Calculations and observations on salt water intrusion, II. Validation of a geochemical model with laboratory experiments. J Hydrol, 120, 225–250.

Appelo, C.A.J., Willemsen, A., Beekman, H.E., & Griffioen, J. (1990). Geochemical calculations and observations on salt water intrusions. II. Validation of a geochemical model with laboratory experiments. Journal of Hydrology, 120(1-4), 225–250. https://doi.org/10.1016/0022-1694(90)90151-M

Ayenew, T., Fikre, S., Wisotzky, F., Demlie, M., & Wohnlich, S. (2009a). Hierarchical cluster analysis of hydrochemical data as a tool for assessing the evolution and dynamics of groundwater across the Ethiopian rift. International Journal of Physical Sciences, 4(2), 76–90.

Ayenew, T., Fikre, S., Wisotzky, F., Demlie, M., & Wohnlich, S. (2009b). Hierarchical cluster analysis of hydrochemical data as a tool for assessing the evolution and dynamics of groundwater across the Ethiopian rift. International Journal of Physical Sciences, 4(2), 76–90.

Barkat, A., Bouaicha, F., Bouteraa, O., Mester, T., Ata, B., Balla, D., Rahal, Z., & Szabó, G. (2021). Assessment of Complex Terminal Groundwater Aquifer for Different Use of Oued Souf Valley (Algeria) Using Multivariate Statistical Methods, Geostatistical Modeling, and Water Quality Index. Water, 13(11), 1609. https://doi.org/10.3390/w13111609

Barkat, A., Bouaicha, F., Mester, T., Debabeche, M., & Szabó, G. (2022). Assessment of Spatial Distribution and Temporal Variations of the Phreatic Groundwater Level Using Geostatistical Modelling: The Case of Oued Souf Valley-Southern East of Algeria. Water, 14(9), 1415. https://doi.org/10.3390/w14091415

Belkhiri, L., Boudoukha, A., Mouni, L., & Baouz, T. (2010a). Application of multivariate statistical methods and inverse geochemical modeling for characterization of groundwater — A case study: Ain Azel plain (Algeria). Geoderma, 159(3-4), 390–398. https://doi.org/10.1016/j.geoderma.2010.08.016

Belkhiri, L., Boudoukha, A., Mouni, L., & Baouz, T. (2010b). Application of multivariate statistical methods and inverse geochemical modeling for characterization of groundwater—a case study: Ain Azel plain (Algeria). Geoderma, 159(3-4), 390–398.

Blés, J. L., & Fleury, J. J. (1970a). Carte géologique de l'Algérie au 1/50000: feuille n 178, Morsott, avec notice explicative détaillée. Service De Cartes Géologique Et Sonatrach, Division D'hydrocarbure. Direction Explorations, Alger, Algerie.

Blés, J.L., & Fleury, J.J. (1970b). Carte géologique de l'Algérie au 1/50000: feuille n 178, Morsott, avec notice explicative détaillée *"Geological map of Algeria at 1/50000: sheet n 178, Morsott, with detailed explanatory note"* Service De Cartes Géologique Et Sonatrach, Division D'hydrocarbure. Direction Explorations, Alger, Algerie.

Bouaicha, F., Dib, H., Bouteraa, O., Manchar, N., Boufaa, K., Chabour, N., & Demdoum, A. (2019). Geochemical assessment, mixing behavior and environmental impact of thermal waters in the Guelma geothermal system, Algeria. Acta Geochimica, 38(5), 683–702. https://doi.org/10.1007/s11631-019-00324-2

Bouteraa, O., Mebarki, A., Bouaicha, F., Nouaceur, Z., & Laignel, B. (2019). Groundwater quality assessment using multivariate analysis, geostatistical modeling, and water quality index (WQI): a case of study in the Boumerzoug-El Khroub valley of Northeast Algeria. Acta Geochimica, 38(6), 796–814. https://doi.org/10.1007/s11631-019-00329-x

Busico, G., Cuoco, E., Kazakis, N., Colombani, N., Mastrocicco, M., Tedesco, D., & Voudouris, K. (2018). Multivariate statistical analysis to characterize/discriminate between anthropogenic and geogenic trace elements occurrence in the Campania Plain, Southern Italy. Environmental Pollution (Barking, Essex : 1987), 234, 260–269. https://doi.org/10.1016/j.envpol.2017.11.053

Călmuc, V. A., Călmuc, M., Ţopa, C. M., Timofti, M., Iticescu, C., & Georgescu, L. P. (2018). Various methods for calculating the water quality index. Annals of the "Dunarea De Jos" University of Galati. Fascicle II, Mathematics, Physics, Theoretical Mechanics, 41(1), 171–178. https://doi.org/10.35219/ann-ugal-math-phys-mec.2018.2.09

Chabour, N., Dib, H., Bouaicha, F., Bechkit, M. A., & Messaoud Nacer, N. (2021). A conceptual framework of groundwater flowpath and recharge in Ziban aquifer: south of Algeria. Sustainable Water Resources Management, 7(1), 36p. https://doi.org/10.1007/s40899-020-00483-8

Chelih, F., Fehdi, C., & Khan, S. (2018). Characterization of the Hammamet basin aquifer (North-East of Algeria) through geochemical and geostructural methods and analysis. Journal of Water and Land Development, 37(1), 39–48. https://doi.org/10.2478/jwld-2018-0023

Chemseddine, F., Dalila, B., & Fethi, B. (2015). Characterization of the main karst aquifers of the Tezbent Plateau, Tebessa Region, Northeast of Algeria, based on hydrogeochemical and isotopic data. Environmental Earth Sciences, 74(1), 241–250. https://doi.org/10.1007/s12665-015-4480-x

Dixon, W., & Chiswell, B. (1992a). The use of hydrochemical sections to identify recharge areas and saline intrusions in alluvial aquifers, southeast Queensland, Australia. Journal of Hydrology, 135(1-4), 259–274.

Dixon, W., & Chiswell, B. (1992b). The use of hydrochemical sections to identify recharge areas and saline intrusions in alluvial aquifers, southeast Queensland, Australia. Journal of Hydrology, 135(1-4), 259–274. https://doi.org/10.1016/0022-1694(92)90091-9

Drias, T., Khedidja, A., Belloula, M., Badraddine, S., & Saibi, H. (2020). Groundwater modelling of the Tebessa-Morsott alluvial aquifer (northeastern Algeria): A geostatistical approach. Groundwater for Sustainable Development, 11, 100444. https://doi.org/10.1016/j.gsd.2020.100444

Farnham, I.M., Johannesson, K.H., Singh, A.K., Hodge, V.F., & Stetzenbach, K.J. (2003). Factor analytical approaches for evaluating groundwater trace element chemistry data. Analytica Chimica Acta, 490(1-2), 123–138. https://doi.org/10.1016/S0003-2670(03)00350-7

Fehdi, C., Rouabhia, A., Baali, F., & Boudoukha, A. (2009). The hydrogeochemical characterization of Morsott-El Aouinet aquifer, Northeastern Algeria. Environmental Geology, 58(7). https://doi.org/10.1007/s00254-008-1667-4

Fehdi, C., Rouabhia, A., Mechai, A., Debabza, M., Abla, K., & Voudouris, K. (2016). Hydrochemical and microbiological quality of groundwater in the Merdja area, Tébessa, North-East of Algeria. Applied Water Science, 6(1), 47–55. https://doi.org/10.1007/s13201-014-0209-3

Foued, B., Hénia, D., Lazhar, B., Nabil, M., & Nabil, C. (2017). Hydrogeochemistry and geothermometry of thermal springs from the Guelma region, Algeria. Journal of the Geological Society of India, 90(2), 226–232. https://doi.org/10.1007/s12594-017-0703-y

Gayar, A. E., & Hamed, Y. (2018). Climate Change and Water Resources Management in Arab Countries. In A. Kallel, M. Ksibi, H. Ben Dhia, & N. Khélifi (Eds.), Advances in Science, Technology & Innovation. Recent Advances in Environmental Science from the Euro-Mediterranean and Surrounding Regions (Vol. 100, pp. 89–91). Springer International Publishing. https://doi.org/10.1007/978-3-319-70548-4_31

Gebrehiwot, T., van der Veen, A., & Maathuis, B. (2011). Spatial and temporal assessment of drought in the Northern highlands of Ethiopia. International Journal of Applied Earth Observation and Geoinformation, 13(3), 309–321.

Giri, A., Bharti, V. K., Kalia, S., Kumar, K., Raj, T., & Chaurasia, O. P. (2019). Utility of multivariate statistical analysis to identify factors contributing river water quality in two different seasons in cold-arid high-altitude region of Leh-Ladakh, India. Applied Water Science, 9(2). https://doi.org/10.1007/s13201-019-0902-3

Goher, M. E., Abdo, M. H., Mangood, A. H., & Hussein, M. M. (2015). Water quality and potential health risk assessment for consumption of Oreochromis niloticus from El-Bahr El-Pharaony Drain, Egypt. Fresenius Environ. Bull, 24(11), 3590–3602.

Güler, C., & Thyne, G.D. (2004). Hydrologic and geologic factors controlling surface and groundwater chemistry in Indian Wells-Owens Valley area, southeastern California, USA. Journal of Hydrology, 285(1-4), 177–198. https://doi.org/10.1016/j.jhydrol.2003.08.019

Hamad, A., Baali, F., Hadji, R., Zerrouki, H., Besser, H., Mokadem, N., Legrioui, R., & Hamed, Y. (2018). Hydrogeochemical characterization of water mineralization in Tebessa-Kasserine karst system (Tuniso-Algerian Transboundry basin). Euro-Mediterranean Journal for Environmental Integration, 3(1). https://doi.org/10.1007/s41207-017-0045-6

Hamad, A., Hadji, R., Bâali, F., Houda, B., Redhaounia, B., Zighmi, K., Legrioui, R., Brahmi, S., & Hamed, Y. (2018). Conceptual model for karstic aquifers by combined analysis of GIS, chemical, thermal, and isotopic tools in Tuniso-Algerian transboundary basin. Arabian Journal of Geosciences, 11(15). https://doi.org/10.1007/s12517-018-3773-2

Karami, S., Madani, H., Katibeh, H., & Fatehi Marj, A. (2018). Assessment and modeling of the groundwater hydrogeochemical quality parameters via geostatistical approaches. Applied Water Science, 8(1). https://doi.org/10.1007/s13201-018-0641-x

Kassahun, Y., & Kebedee, T. (2012). Application of Principal Component Analysis in Surface Water Quality Monitoring. In P. Sanguansat (Ed.), Principal Component Analysis - Engineering Applications. InTech. https://doi.org/10.5772/38049

King, S. F., Merle, A., Morisi, S., Shimizu, Y., & Tanimoto, M. (2014). Neutrino Mass and Mixing: from Theory to Experiment. New Journal of Physics 16(4), 045018. https://doi.org/10.48550/arXiv.1402.4271

Kouadra, R., Demdoum, A., Chabour, N., & Benchikh, R. (2019). The use of hydrogeochemical analyses and multivariate statistics for the characterization of thermal springs in the Constantine area, Northeastern Algeria. Acta Geochimica, 38(2), 292–306. https://doi.org/10.1007/s11631-018-0298-z

Legrioui, R., Baali, F., Abdeslam, I., Hamad, A., Audra, P., Cailhol, D., & Jaillet, S. (2020). Hydrochemical and Isotopic Characterization of Karst Aquifer in the Region of Tebessa, Northeast Algeria. In C. Bertrand, S. Denimal, M. Steinmann, & P. Renard (Eds.), Advances in Karst Science. Eurokarst 2018, Besançon (pp. 223–231). Springer International Publishing. https://doi.org/10.1007/978-3-030-14015-1_25

Loh, Y. S. A., Akurugu, B. A., Manu, E., & Aliou, A.-S. (2020). Assessment of groundwater quality and the main controls on its hydrochemistry in some Voltaian and basement aquifers, northern Ghana. Groundwater for Sustainable Development, 100296. https://doi.org/10.1016/j.gsd.2019.100296

Magaritz, M., Nadler, A., Koyumdjisky, H., & Dan, J. (1981a). The use of Na/Cl ratios to trace solute sources in a semiarid zone. Water Resources Research, 17(3), 602–608. https://doi.org/10.1029/WR017i003p00602

Magaritz, M., Nadler, A., Koyumdjisky, H., & Dan, J. (1981b). The use of Na/Cl ratios to trace solute sources in a semiarid zone. Water Resources Research, 17(3), 602–608.

Mahapatra, S.S., Sahu, M., Patel, R.K., & Panda, B.N. (2012). Prediction of Water Quality Using Principal Component Analysis. Water Quality, Exposure and Health, 4(2), 93–104. https://doi.org/10.1007/s12403-012-0068-9

Mishra, A. (2010). Assessment of water quality using principal component analysis: A case study of the river Ganges. Journal of Water Chemistry and Technology, 32(4), 227–234. https://doi.org/10.3103/s1063455x10040077

Paiu Mădălina, & Breabăn Iuliana Gabriela. (2014). Water quality index – an instrument for water resources management. https://doi.org/10.13140/2.1.3736.3203

Parkhurst, D.L., & Appelo, C.A.J. (1999a). User's guide to PHREEQC (Version 2): A computer program for speciation, batch-reaction, one-dimensional transport, and inverse geochemical calculations. Advance online publication. https://doi.org/10.3133/wri994259

Parkhurst, D.L., & Appelo, C.A.J. (1999b). User's guide to PHREEQC (Version 2): A computer program for speciation, batch-reaction, one-dimensional transport, and inverse geochemical calculations. Water-Resources Investigations Report, 99(4259), 312.

Piper, A.M. (1944). A Graphic Procedure in the Geochemical Interpretation of Water-Analyses. Eos, Transactions American Geophysical Union, 25, 914-928. http://dx.doi.org/10.1029/TR025i006p00914

Rafighdoust, Y., Eckstein, Y., Harami, R.M., Gharaie, M.H.M., & Mahboubi, A. (2016a). Using inverse modeling and hierarchical cluster analysis for hydrochemical characterization of springs and Talkhab River in Tang-Bijar oilfield, Iran. Arabian Journal of Geosciences, 9(3), 241.

Rafighdoust, Y., Eckstein, Y., Harami, R. M., Gharaie, M. H. M., & Mahboubi, A. (2016b). Using inverse modeling and hierarchical cluster analysis for hydrochemical characterization of springs and Talkhab River in Tang-Bijar oilfield, Iran. Arabian Journal of Geosciences, 9(3), 2881. https://doi.org/10.1007/s12517-015-2129-4

Raiber, M., White, P.A., Daughney, C.J., Tschritter, C., Davidson, P., & Bainbridge, S.E. (2012a). Three-dimensional geological modelling and multivariate statistical analysis of water chemistry data to analyse and visualise aquifer structure and groundwater composition in the Wairau Plain, Marlborough District, New Zealand. Journal of Hydrology, 436, 13–34.

Raiber, M., White, P.A., Daughney, C.J., Tschritter, C., Davidson, P., & Bainbridge, S.E. (2012b). Three-dimensional geological modelling and multivariate statistical analysis of water chemistry data to analyse and visualise aquifer structure and groundwater composition in the Wairau Plain, Marlborough District, New Zealand. Journal of Hydrology, 436-437(3), 13–34. https://doi.org/10.1016/j.jhydrol.2012.01.045

Rouabhia, A., Baali, F., & Fehdi, C. (2010). Impact of agricultural activity and lithology on groundwater quality in the Merdja area, Tebessa, Algeria. Arabian Journal of Geosciences, 3(3), 307–318. https://doi.org/10.1007/s12517-009-0087-4

Sedrati, N., & Djabri, L. (2014). Contribution of hydrochemistry to the characterization and assessment of groundwater resources: the case of Tebessa alluvial aquifer (Algeria). Proceedings of the International Association of Hydrological Sciences, 364, 458–463. https://doi.org/10.5194/piahs-364-458-2014

Shrestha, S., & Kazama, F. (2007). Assessment of surface water quality using multivariate statistical techniques: A case study of the Fuji river basin, Japan. Environmental Modelling & Software, 22(4), 464–475.

Shweta, S. (2013). Dental abscess: A microbiological review. Dental Research Journal, 10(5), 585.

Tardy, Y. (1971). Characterization of the principal weathering types by the geochemistry of waters from some European and African crystalline massifs. Chemical Geology, 7(4), 253–271.

Tyagi, S., Sharma, B., Singh, P., & Dobhal, R. (2020). Water Quality Assessment in Terms of Water Quality Index. American Journal of Water Resources, 1(3), 34–38. https://doi.org/10.12691/ajwr-1-3-3

Valder, J. F., Long, A. J., Davis, A. D., & Kenner, S. J. (2012). Multivariate statistical approach to estimate mixing proportions for unknown end members. Journal of Hydrology, 460-461, 65–76. https://doi.org/10.1016/j.jhydrol.2012.06.037

Vila, J.M. (1980). La chine alpine d'algérie oriontale et des confins Algéro-Tunisiens *"The Alpine chain of eastern Algeria and the Tunisian Algerian borders".* Doctoral thesis. Paris VI university. Orsay. France

Ward Jr, J. H. (1963). Hierarchical grouping to optimize an objective function. Journal of the American Statistical Association, 58(301), 236–244.

WHO (2011). Guidelines for Drinking-Water Quality. WHO Chronicle, 38, 104-108.

Wold, S., Esbensen, K., & Geladi, P. (1987). Principal component analysis. Chemometrics and Intelligent Laboratory Systems, 2(1-3), 37–52. https://doi.org/10.1016/0169-7439(87)80084-9

Xanthopoulos, P., Pardalos, P. M., & Trafalis, T. B. (2013). Principal component analysis. In Robust data mining (pp. 21–26). Springer.

Yang, H., Xiao, Y., Hao, Q., Wang, L., Zhang, Y., Liu, K., Zhu, Y., Liu, G., Yin, S., & Xie, Z. (2023). Geochemical characteristics, mechanisms and suitability for sustainable municipal and agricultural water supply of confined groundwater in central North China Plain. Urban Climate, 49, 101459. https://doi.org/10.1016/j.uclim.2023.101459

Zereg, S., Boudoukha, A., & Benaabidate, L. (2018). Impacts of natural conditions and anthropogenic activities on groundwater quality in Tebessa plain, Algeria. Sustainable Environment Research, 28(6), 340–349. https://doi.org/10.1016/j.serj.2018.05.003